

Design of an Efficient Tin Selenide-Based Ternary Nanocomposite Electrode for Simultaneous Determination of Paracetamol, Tryptophan, and Caffeine

Eagambaram Murugan* and Kalpana Kumar

Cite This: *ACS Omega* 2022, 7, 35486–35495

Read Online

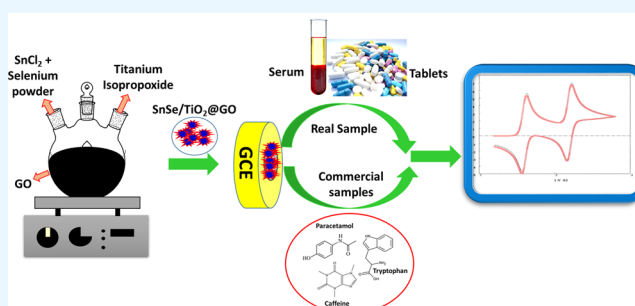
ACCESS |

Metrics & More

Article Recommendations

Supporting Information

ABSTRACT: Electrochemical sensors play an essential role in the medical arena through assessing the drug quality and diagnosing diseases. The design of sensors relies on the electroactive properties of the material meticulously chosen to modify the electrode. Here in this work, a facile ternary SnSe/TiO₂@GO electroactive nanocomposite was prepared using tin selenide (SnSe) in combination with titanium dioxide (TiO₂) embedded on graphene oxide (GO). The ternary nanocomposite was characterized by X-ray diffraction, Raman, FT-IR, and X-ray photoelectron spectroscopy, energy dispersive analysis, and scanning electron microscopy. The ternary nanocomposite was then drop-coated on the GC electrode to form the SnSe/TiO₂@GO-GC electrode. Its electrochemical activity was demonstrated for simultaneous determination of paracetamol, tryptophan, and caffeine. The synergetic interaction of the components and their innate virtue showed enriched electrocatalytic activity such as a decrease in overpotential, enhancement in electron transfer, greater sensing ability and selectivity, wide linear range, and low detection limit toward the chosen analytes. Broad linear ranges of concentrations, 0.0089–410, 0.0136–87.66, and 0.0160–355 μM, with detection limits of 0.0030, 0.0053, and 0.0065 μM for paracetamol, tryptophan, and caffeine, respectively, were noticed. The electrode also displayed high selectivity, stability, repeatability, and reproducibility. Importantly, the study was successful for detection and quantification of the above components in real samples of blood serum, pharmaceutical formulations, and beverages.



INTRODUCTION

There has been a huge demand for sensitive electrodes/electrochemical sensors in the medical arena for the rapid analysis of complex lifesaving drugs and real blood samples. Graphene oxide (GO) is a derivative of graphene and possesses all the properties of graphene as well as some exceptional properties such as multiple oxygen groups, hydrophilicity, and controllable electronic properties. These functional groups make it advantageous for fabricating several functional devices, like photovoltaics, fuel cells, sensors, and photodetectors.^{1–3} Fabrication of such two-dimensional (2D) devices has accelerated interest in other 2D materials such as metal chalcogenides with some unusual properties. Indeed, metal chalcogenides have been utilized in catalysis, solar cell applications, and lithium-ion batteries due to their exclusive properties such as greater specific surface area and exotic electronic properties, which play a vital role in energy storage, sensing, and field-emitting applications.^{4,5} Particularly, tin-based chalcogenides such as SnS, SnSe, and SnTe have a wide range of applications owing to their low band gap and active adsorbing sites. Among the tin chalcogenides, p-type tin selenide (SnSe) is nontoxic and cheap and its constituent elements are abundant in nature, which helps significantly

improve their worth in sustainable energy-related applications.⁶ Similarly, metal oxides such as iron oxide⁷ and TiO₂ have also been employed for various applications particularly as electrocatalytic material for sensing of various pollutants, drugs, dyes, and metals discharged from organic/pharmaceutical industries.^{8,9} The integration of these materials into GO can improve the conductivity and electrochemical stability. This enhanced behavior cannot be achieved in a single component, and therefore, the resulting ternary nanocomposite will be a promising candidate for electrochemical application. Murugan et al. reported a glucose sensor using a modified GC electrode with MWCNT and Au nanoparticles¹⁰ and also reported a SnS/TiO₂@GO ternary nanocomposite for electrochemical sensing of drugs present together in biosamples.¹¹ To analyze the tin chalcogenides, it was decided to synthesize a ternary nanocomposite using SnSe in

Received: December 27, 2021

Accepted: February 18, 2022

Published: September 27, 2022



combination with GO and TiO₂ where GO acts as a matrix for anchoring active materials to maintain electrical contact throughout the composite. There is no study reporting the synergistic effect of SnSe with GO and TiO₂ especially for electrocatalytic sensing applications. Hence, to examine the electrochemical property of the prepared ternary nanocomposite, a new electrode, SnSe/TiO₂@GO-GC, was fabricated. In the medical field, paracetamol (Para) and caffeine (Caf) are prominent life-saving drugs and they are often used in combination.

To mention briefly, Para is a phenolic compound that becomes one of the main drugs in day-to-day human's life owing to its antipyretic and analgesic activities.^{12,13} In addition, Para has effective therapeutic capacity in neurodegenerative conditions such as Parkinson's and Alzheimer's diseases.¹⁴ Nevertheless, if more than the usual therapeutic dose is used, such as more than 20 μg/mL, Para can accumulate in the body and kill the liver, skin, and pancreas.¹⁵ Moreover, after administration of this drug, a major portion is used to treat diseases but little amount is excreted in urine,¹⁶ and thus, it becomes a pollutant to soils and waters.¹⁷ Caf is an active alkaloid stimulant to the central nervous and cardiovascular systems. It is a major ingredient for pharmaceutical and food industries such as coffee, Coca-Cola, cola nuts, and tea.¹¹ In addition, intake of Caf gives more benefits such as neuroprotective and metabolic functions and it promotes diuresis and gastric acid secretion.¹⁸ Caf is used to treat nasal congestion, asthma, and headache, facilitate weight loss, and improve athletic endurance.¹⁹ However, when excessively consumed, for instance, 180 mg/day, it can cause adverse mutation effects, inhibition of DNA repair, heart diseases, and cancer. Similarly, tryptophan (Trp) exists in human nutrition and herbivores due to its essential amino acid character. It acts as a vital element to balance the nitrogen level for indispensable growth of humans.²⁰ The human body is not synthesizing Trp, which is present at a scarce level in vegetables. Hence, it must be taken from food and pharmaceutical formulations.²¹ The excess intake such as 7.47 nmol/mL or improper metabolism of this amino acid may result in schizophrenia, hallucinations, and delusions, and its oxidation products can induce certain cancers.^{22,23} It is in this circumstance that it is necessary to sense and quantify all of them, particularly in pharmaceutical formulations. When these components are higher or lower than the required limit in the drug formulations, obviously, they severely affect the patients. Therefore, effective sensing and accurate quantification of these components in real blood samples could lead to solving the above said problems. More specifically, in the previous study, we have reported a smart electrode, viz., SnS/TiO₂@GO, a ternary nanocomposite-coated GCE, and demonstrated it to be successful for simultaneous detection and quantification of medically valuable drugs including Para, Caf, and Trp through a single experiment.¹¹ In continuation to that, in this work, a novel SnSe/TiO₂@GO ternary nanocomposite was synthesized via a superficial technique and an electrochemical sensing platform was constructed for sensitive determination of Para, Caf, and Trp. The resulting electrochemical sensor showed a low-slung detection limit, extensive linear range, and the practical applicability in human serum with satisfactory results.

EXPERIMENTAL SECTION

Reagents. All substances were obtained from Sigma-Aldrich (India) and used: graphite powder, titanium isopropoxide, tryptophan, caffeine, paracetamol, hydrazine hydrate, selenium powder, tin(II) chloride dihydrate, HPLC water, ethylenediamine, sodium dihydrogen phosphate, and disodium hydrogen phosphate. Red Bull, Dolopar, L-tryptophan, and tea pack were obtained from a local market and used.

Synthesis of Tin Selenide. Based on a previous report,²⁴ tin selenide was prepared through a solvothermal method. Initially, 0.45 g of SnCl₂·2H₂O was dissolved in 15 mL of ethylenediamine. Then, 0.15 g of selenium powder was added to the resulting solution and stirred for 25 min. The suspension became dark brown and then was alienated to the Teflon-lined autoclave (100 mL). Then, ethylenediamine was added to it until the volume of the autoclave reached 75 mL. The autoclave was closed, heated at 190 °C for 8 h in an oven, and then allowed to cool down to room temperature. The resulting product was filtered under suction and washed with DD water followed by absolute ethanol for three times each. The residue was then dried at 80 °C and calcined at 450 °C for 6 h to get tin selenide nanoparticles.

Synthesis of SnSe/TiO₂@GO. To oxidize graphite into graphene oxide (GO), a modified Hummer's method²⁵ was applied. GO (0.05 g) was ultrasonicated in 25 mL of DD water and then SnSe (0.0015 g) and titanium isopropoxide (0.2 mL) were added to it under stirring. After half an hour, the resulting solution was poured into a 100 mL autoclave, the reaction was carried out for 9 h at 120 °C, and the thus-obtained black product was filtered under suction and washed with DD water. The observed residue was dried at 85 °C and calcined at 530 °C for 4 h to obtain the SnSe/TiO₂@GO ternary nanocomposite.

Modification of GC Electrodes Using the SnSe/TiO₂@GO Ternary Nanocomposite. Before modification of the GC electrode, it was polished with alumina powders with grain sizes of 0.05 μm and then 0.3 μm. The GC electrode was then washed with water and ethanol and dried at ambient temperature. Then, the SnSe/TiO₂@GO ternary nanocomposite (10 mg) was dispersed in 10 mL of water to obtain a stock solution. The stock solution was sonicated and 5 μL of it was pipetted out, drop-coated on the pretreated GC electrode, and dried at room temperature to get the SnSe/TiO₂@GO-GC electrode. In the same way, the control electrodes such as GO-GC, SnSe-GC, and TiO₂-GC were also fabricated following the same procedure.

Preparation of Real Samples and Their Measurement Procedures. To obtain the serum sample, human blood was coagulated (4 °C) and centrifuged. Further, the obtained serum (1 mL) was then added to 20 mL of 0.1 M phosphate buffer solution (PBS) in a volumetric cell and labeled as sample 1. Sample 2 was prepared by mixing the serum with 5 μM Panadol extra (Para & Caf source) and L-tryptophan (500 mg) tablet and subsequent simultaneous determination was carried out. In the same way, sample 3 was also prepared by dissolving 5 μM Paracip-650 capsule (paracetamol source), a 5 μM L-tryptophan (500 mg) tablet (tryptophan source), and a 5 wt % 3 roses tea solution (Caf source) and a similar experiment was carried out. The HPLC analysis was also carried out for sample 2 with a C18 column in which a mixture of acetonitrile and phosphate buffer (60:40 (v/v)) solution

acts as a mobile phase, and the subsequent elution was observed using a 254 nm UV detector.

RESULTS AND DISCUSSION

SEM and EDX Analysis. To study the morphology of the SnSe/TiO₂@GO ternary nanocomposite, GO, SnSe, and TiO₂ were examined using SEM (Figure 1a–d), respectively. The

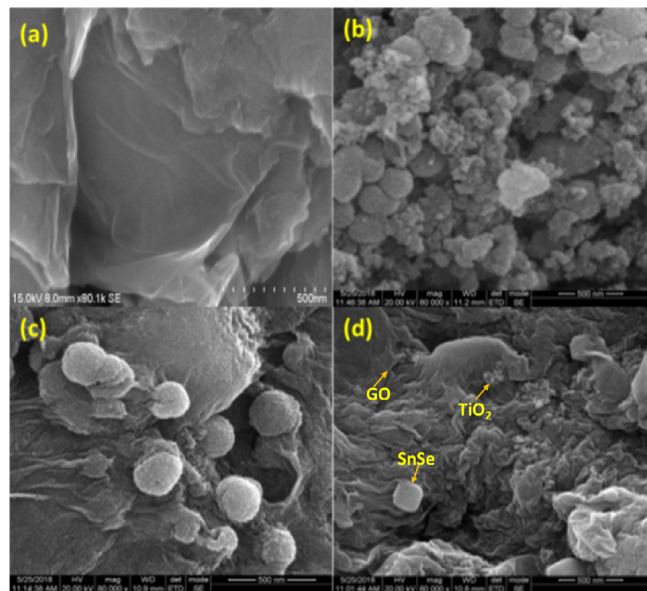


Figure 1. SEM images of (a) GO, (b) SnSe nanoparticles, and (c, d) the SnSe/TiO₂@GO ternary nanocomposite.

surface morphology of GO showed the absence of aggregates due to its hydrophilic nature (Figure 1a). The SEM image (Figure 1b) of SnSe nanoparticles showed aggregates of spheres. These results are in good agreement with a previous report.²⁶ The SEM image (Figure 1c,d) of the SnSe/TiO₂@GO ternary nanocomposite depicted spheres of different sizes distinctly entrapped in the stacked layer structure with the average size range from 40 to 60 nm, which is due to the distinct sizes of SnSe and TiO₂.

The EDX results of the SnSe/TiO₂@GO ternary nanocomposite also confirm the presence of Sn, Se, O, Ti, and C and their distribution is verified through elemental mapping (Figure S1a). Similarly, the EDX spectrum of SnSe (Figure S1b) also reveals that the average Se:Sn atomic percentage ratio is 50.33:45.07, indicating the correct stoichiometry of SnSe. This is in consensus with the XRD results.

XRD Analysis. Figure 2a–c presents the XRD results of GO, SnSe, and the SnSe/TiO₂@GO ternary nanocomposite. Figure 2a shows a diffraction peak of GO at $2\theta = 11.14^\circ$.²⁷ SnSe (Figure 2b) showed peaks at $2\theta = 30.25^\circ, 42.61^\circ, 52.23^\circ,$ and 67.34° , which correspond to the orthorhombic phase of SnSe (JCPDS no. 89-0236).²⁸ In addition, the high intensity confirms the high crystalline nature of the spheres. Similarly, the SnSe/TiO₂@GO ternary nanocomposite also showed diffraction peaks corresponding to GO at 10.2° , SnSe at 30.24° and 67.19° , and TiO₂ at $25.17^\circ, 38.39^\circ,$ and 48.26° .²⁹ The observed peak positions of the ternary nanocomposite were shifted to a lower angle due to the content of SnSe/TiO₂ (Figure 2c). The mean sizes of SnSe and TiO₂ crystal were observed as 27 and 17.35 nm, respectively.

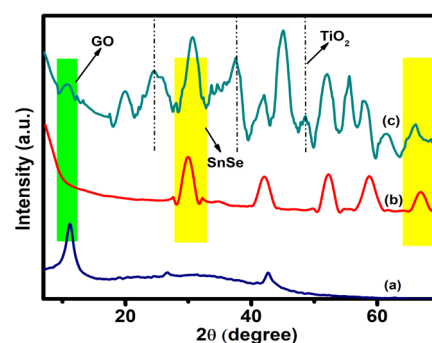


Figure 2. XRD pattern of (a) GO, (b) SnSe, and (c) the SnSe/TiO₂@GO ternary nanocomposite.

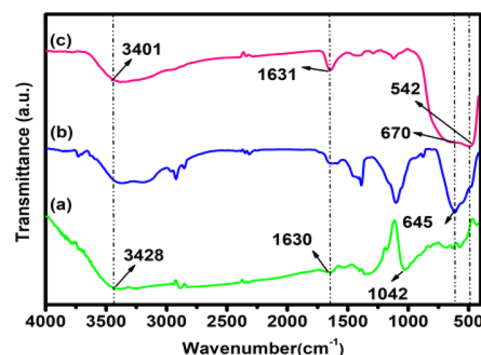


Figure 3. FT-IR spectra of (a) GO, (b) SnSe, and (c) the SnSe/TiO₂@GO ternary composite.

FT-IR Analysis. The FT-IR spectra of GO, SnSe, and the SnSe/TiO₂@GO ternary nanocomposite are shown in Figure 3a–c. The broad peak at 3427 cm^{-1} is assigned to O–H_{str} of GO (Figure 3a). Another set of peaks observed at 1042 and 1630 cm^{-1} were due to C–O and C=C groups, respectively, of GO. Corresponding to that, the SnSe/TiO₂@GO ternary nanocomposite (Figure 3c) showed OH vibration at 3407 cm^{-1} and C–O and C=C vibrations at 1030 and 1631 cm^{-1} , respectively. In addition, SnSe showed its Sn–Se stretching vibration at 645 cm^{-1} (Figure 3b), indicating the formation of an orthogonal structure.³⁰ Similarly, the SnSe/TiO₂@GO ternary nanocomposite also gives good agreement with SnSe by the appearance of a peak at 670 cm^{-1} . In addition, the SnSe/TiO₂@GO ternary nanocomposite also showed a broad band at 542 cm^{-1} corresponding to Ti–O–Ti bond vibration³¹ (Figure 3c). Similarly, other two peaks at 1633 and 3424 cm^{-1} are ascribed to Ti³⁺–O–Ti⁴⁺ bond bending and stretching vibration modes of the OH group, respectively. In the composite, there is broadening below 600 cm^{-1} , which may be due to the formation of Ti–O–C bonds,^{32,33} and these Ti–O–C bonds strongly suggest the formation of chemical bonds between TiO₂ and GO nanoparticles.

Raman Spectral Analysis. The Raman spectra of the SnSe/TiO₂@GO ternary nanocomposite, GO, and SnSe are depicted in Figure 4a–c. The spectrum of the SnSe/TiO₂@GO ternary nanocomposite (Figure 4a) showed a pair of peaks at 1350 and 1579 cm^{-1} corresponding to D and G bands of GO. In addition, another set of peaks occurred at 108 and 129 cm^{-1} due to B_{3g} and A_g modes,³⁴ respectively, of the orthorhombic structure of SnSe (Figure 4b). The peak at 395 cm^{-1} confirms TiO₂ availability³⁵ in the SnSe/TiO₂@GO ternary nanocomposite. All these results confirm the

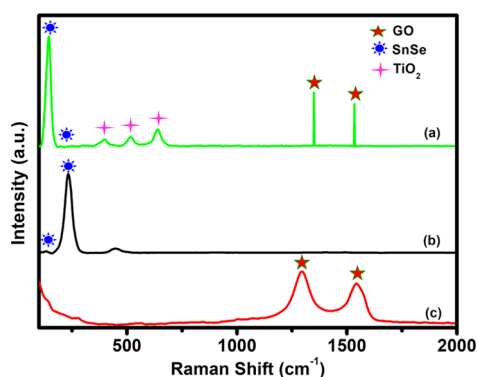


Figure 4. Raman spectra of (a) the SnSe/TiO₂@GO ternary nanocomposite, (b) SnSe, and (c) GO.

coexistence of the aforementioned compounds in the composite.

XPS Analysis. The element electronic states and surface composition of the SnSe/TiO₂@GO ternary nanocomposite are studied by XPS and shown in Figure 5. Deconvolution of the C 1s spectrum in the SnSe/TiO₂@GO ternary nanocomposite (Figure 5b) showed peaks at 282.21, 284.4, 285.2, 285.8, 287.2, and 289.4 eV ascribed to the C–Sn, C–Ti, C–C, C=C, C–O, and C=O bonds, respectively.^{36,37} The presence of C–Ti bonds strongly confirms the deposition of TiO₂ nanoparticles on GO via interfacial bonding. The deconvoluted Se 3d spectrum (Figure 5c) showed two major bands at 54.2 and 55 eV corresponding to the Se–Sn bonds of the spheres.³⁸ In addition, Figure 5e shows that two bands centered at 495.7 and 486.6 eV correspond to Sn 3d_{3/2} and Sn 3d_{5/2}, respectively. Similarly, the availability of 3d electronic states of Sn and Se confirms the SnSe stoichiometry. Also, two major peaks for Ti⁴⁺ in TiO₂ (Figure 5d) were observed at 459.4 and 465.7 eV, and they were shifted to higher energy than pristine TiO₂.³⁹ It confirms the electron transfer from TiO₂ to SnSe. Similarly, two minor bands at 460.2 and 466.5 eV represent the formation of Ti–C bonds,³⁷ which give good agreement with

the C 1s result. Particularly, the presence of C–Ti bonding between GO and TiO₂ interface and C–Sn bonding between GO and SnSe interface confirms the formation of the composite. In addition, these interactions can induce the electron transport in the composite.

Electrochemical Performance of the SnSe/TiO₂@GO Ternary Nanocomposite. To verify the electrocatalytic activity of the synthesized SnSe/TiO₂@GO ternary nanocomposite, cyclic voltammetry (CV) and differential pulse voltammetry (DPV) studies were carried out in the presence of Para in 0.1 M phosphate buffer solution (pH 7.2). Further, the efficiency of the SnSe/TiO₂@GO-GC ternary electrode was compared with control electrodes such as bare GC, GO-GC, SnSe-GC, and TiO₂-GC, and the observed results are shown in Figure 6. From the results, it is observed that there is no peak

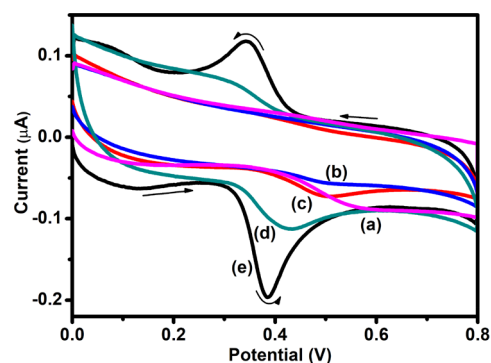


Figure 6. CV curves of oxidation of Para (17 μM) at (a) bare GC, (b) GO-GC, (c) SnSe-GC, (d) TiO₂-GC, and (e) SnSe/TiO₂@GO-GC electrodes in 0.1 M PBS (pH 7.2) (scan rate of 50 mV s^{-1}).

potential in the absence of Para, whereas in the presence of 17 μM Para control electrodes, bare GC and GC-GO exhibited high overpotential, but in the case of SnSe-GC (0.41 and 0.32 V) and TiO₂-GC (0.49 and 0.37 V), relatively low over potentials were observed. Such a performance of SnSe-GC and TiO₂-GC electrodes may be due to the high surface-to-volume

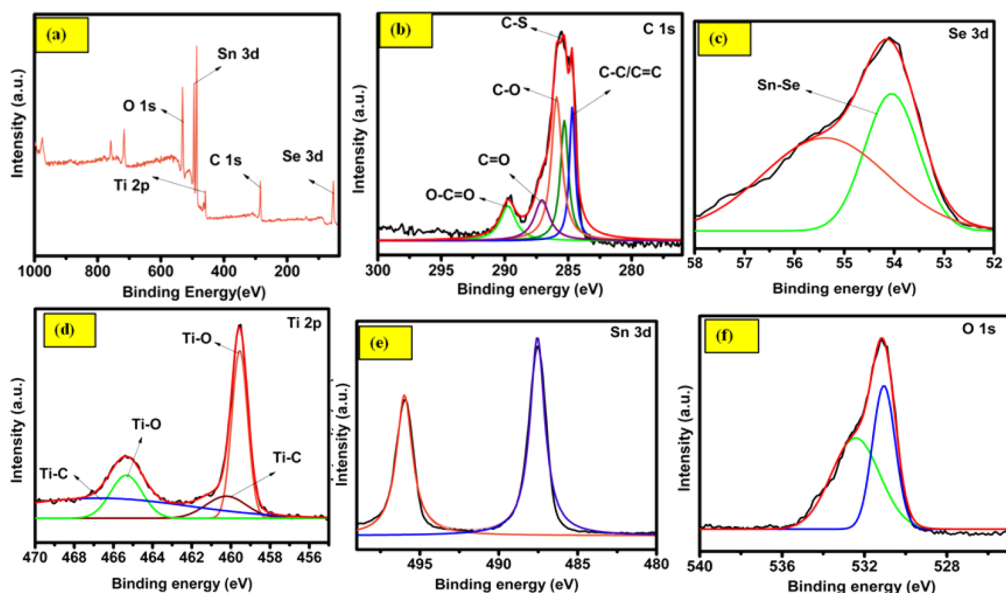


Figure 5. XPS analysis of (a) the SnSe/TiO₂@GO ternary nanocomposite and (b) deconvoluted C 1s, (c) Se 3d (d) Ti 2p, (e) Sn 3d, and (f) O 1s.

ratio. In contrast to it, the SnSe/TiO₂@GO-GC electrode showed peaks with redox behavior at 0.38 and 0.34 V with improved peak currents and thus showed 20 mV lesser oxidation potential than the previous work,¹¹ and this distinction is due to the synergetic effects of the constituents that led to the high electrical conductivity and relatively small band gap of SnSe⁴⁰ and the potent interface of TiO₂.¹¹ In addition, a Lewis acid–base interaction is expected between SnSe and TiO₂, thus leading to a surface assimilation of the electrode, which results in dwindling of bonds and lower oxidation potential.¹¹ In view of the observations, the SnSe/TiO₂@GO-GC electrode has enriched electrocatalytic activity toward Para oxidation, and the mechanism is shown in Scheme S1. On increasing the concentration of Para from 9.1 nM to 296.5 μM (Figure 7), the peak currents were also increasing.

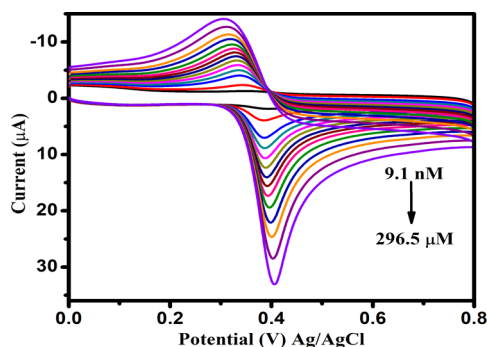


Figure 7. CV curves of different concentrations of Para at the SnSe/TiO₂@GO-GC electrode in 0.1 M PBS (scan rate of 50 mV s⁻¹).

Effect of pH. The electrochemical behavior of the fabricated electrode and analyte peak current can be influenced by the pH of the electrolyte. Due to the involvement of protons in the oxidation of paracetamol reaction, the effect of pH on the peak potential, voltammetric behavior, and peak currents was investigated at the SnSe/TiO₂@GO-GC electrode with a pH range from 5 to 9 (scan rate of 50 mV s⁻¹), and the result is shown in Figure 8a. From the observed CV response, it is observed that there is a shift in Para oxidation potential toward the negative side while increasing the pH, which confirms the direct participation of protons. There exists a linearity between the peak potential and pH (Figure 8b), which is the nearest to the Nernst equation, and the observed equation is $E_{p_{\text{ano}}}/V = -0.0502(\text{pH}) + 0.8290$ ($R = 0.9957$). The results depict that the oxidation reaction involves an equivalent of protons and electrons such as 2 (calculated using

eq 1).¹¹ From the results, it is observed that the maximum oxidation current was observed at pH 7; therefore, it was chosen for further study.

$$E = E_0 - 0.0591\text{pH}/n \quad (1)$$

Effect of Scan Rate. The influence of the scan rate on the SnSe/TiO₂@GO-GC electrode was studied by varying the scan rate from 10 to 100 mV s⁻¹ at 25 μM Para (Figure 9a). The results showed that the anodic current upgrades linearly toward a more positive direction on increasing scan rate.⁴¹ As seen in Figure 9b, the plot of log I_p vs log scan rate showed a linear dependence with the linear regression equation of log I_p (μA) = 0.8448 log ν + 1.6158 ($R^2 = 0.9994$). Plots of log I_p vs log ν showed a slope value of 0.84, indicating that the oxidation reaction that occurs at the SnSe/TiO₂@GO-GC electrode is controlled by the adsorption process.⁴²

The surface coverage concentration of the ternary composite on the GC electrode as well as Para adsorbed on the surface of the SnSe/TiO₂@GO-GC electrode is calculated using Laviron's model (eq 2) since it has an effect on fouling, potential, and interference of other electroactive species. The observed values for SnSe/TiO₂@GO-GC and Para-adsorbed SnSe/TiO₂@GO-GC electrodes are 3.2 and 3.04 nM cm⁻², respectively,⁴³ and thus endorse the better conductivity of the fabricated electrode.

$$I_p = n^2 F^2 A \Gamma \nu / 4RT \quad (2)$$

I_p is the peak current, n is the number of electrons involved, F is the Faraday constant, Γ is the surface coverage concentration, A is the surface area, ν is the scan rate, R is the gas constant, and T is the temperature (K).

The electroactive surface area (A_{real}) and % A_{real} of the SnSe/TiO₂@GO-GC electrode were evaluated through the Randles–Sevcik equation (equation 1)⁴⁴ and they were equal to 0.076 cm² and 92.9%, respectively.

Voltammetric Determination of Paracetamol. DPV was employed to study the effect of concentration of Para on the SnSe/TiO₂@GO-GC electrode due to its high sensitivity and acute resolution in quantitative determination, and the results are shown in Figure 10. The results illustrate that the anodic peak currents of Para gradually increased from 0.0089 to 381 μM with the increase in concentration of Para with the linearity of I_p (10⁻⁶ A) = 0.0993[Para/μM] + 0.0796 ($R^2 = 0.9995$) (Figure 10, inset). The detection limit is calculated using $3\sigma/S$ and it is equal to 0.003 μM.

As discussed earlier, if there is an electrode that can separate the peak potentials of Para, Trp, and Caf simultaneously with

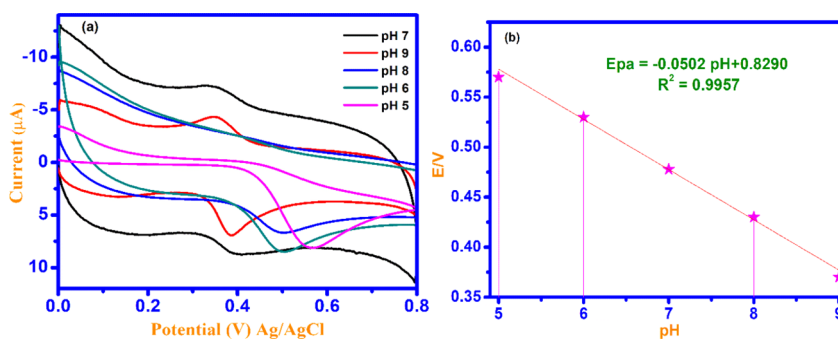


Figure 8. CV curves of (a) pH values from 5 to 9 in 0.1 M PBS at the SnSe/TiO₂@GO-GC electrode and (b) its calibration plot (scan rate of 50 mV s⁻¹).

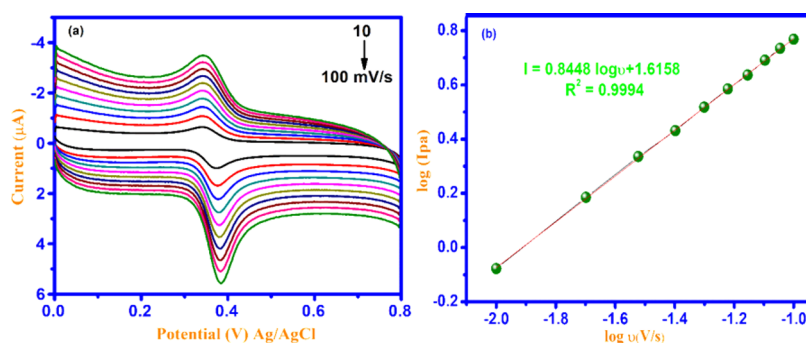


Figure 9. CV curves of (a) various scan rates and (b) calibration plot of $\log I_{pa}$ vs $\log \nu$ at the SnSe/TiO₂@GO-GC electrode.

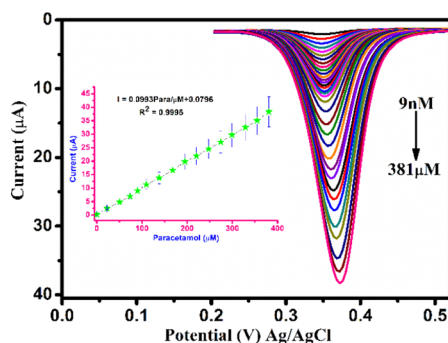


Figure 10. DPV curves of concentration variation of Para in 0.1 M PBS at the SnSe/TiO₂@GO-GC electrode and its calibration plot (inset).

lower potential, it will be a great contribution for the biomedical arena.^{45–47} The main objective of the present study is to evaluate the electrochemical applicability of the electrode in both separate and simultaneous analyses of drugs.

To bring out the selectivity of the electrode, DPV measurements were carried out using the SnSe/TiO₂@GO-GC electrode by changing the concentration of one analyte and keeping the concentration of the others as constant under optimum conditions (Figure 11a–d). In Figure 11a, it is observed that the peak current of Para increases on increasing the Para concentration from 0.0089 to 410 μM , whereas the concentrations of Trp and Caf are 0.0136 and 0.0160 μM , respectively. Similarly, on increasing the concentration of Trp from 0.0136 to 190 μM at a steady concentration of Para and Caf (Figure 11b), a new peak was observed at 1.0 V as discussed earlier.¹¹ Finally, the concentration of Caf varied from 0.0160 to 355 μM at a steady concentration of Para and Trp (Figure 11c). The observed linear equation is as follows.

$$I_{pa} (10^{-6}) = 0.1001[\text{Para}/\mu\text{M}] + 0.0155, R^2 = 0.9993 \text{ (detection limit: } 0.0029 \mu\text{M)}$$

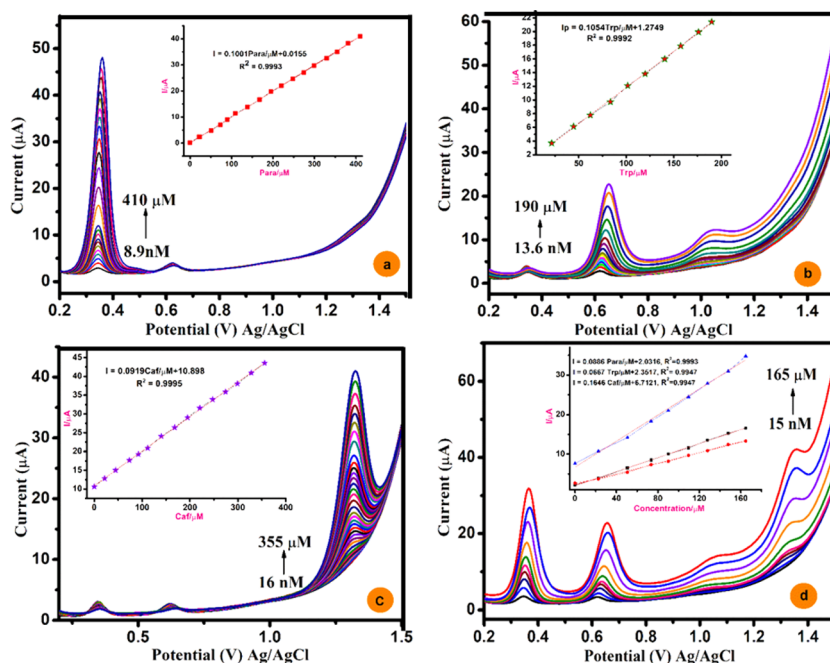


Figure 11. DPV curves of (a) the effect of [Para] with fixed Trp and Caf concentrations and its calibration plot (inset), (b) the effect of [Trp] with fixed Para and Caf concentrations and its calibration plot (inset), (c) the effect of [Caf] with fixed Para and Trp concentrations and its calibration plot (inset), and (d) concomitant determination of Para, Trp, and Caf at various concentrations at the SnSe/TiO₂@GO-GC electrode and their calibration plot (inset).

$$\begin{aligned} I_{pa} (10^{-6}) &= 0.1054[\text{Trp}/\mu\text{M}] + 1.2749, R^2 \\ &= 0.9992 \text{ (detection limit: } 0.0053 \mu\text{M)} \end{aligned}$$

$$\begin{aligned} I_{pa} (10^{-6}) &= 0.0919[\text{Caf}/\mu\text{M}] + 10.8980, R^2 \\ &= 0.9995 \text{ (detection limit: } 0.0065 \mu\text{M)} \end{aligned}$$

The observed DPV curves of concomitant determination of Para, Trp, and Caf exhibited three distinct peak potentials at 0.34, 0.62, and 1.29 V, respectively (Figure 11d). On increasing the concentration of the analytes from 15 nM to 165 μM , the peak currents also increased linearly and the observed linear results were as follows,

$$I_{pa} (10^{-6}) = 0.0886[\text{Para}/\mu\text{M}] + 2.0316 \text{ (} R^2 = 0.9993 \text{)}$$

$$I_{pa} (10^{-6}) = 0.0667[\text{Trp}/\mu\text{M}] + 2.3517 \text{ (} R^2 = 0.9966 \text{)}$$

$$I_{pa} (10^{-6}) = 0.1646[\text{Caf}/\mu\text{M}] + 6.7121 \text{ (} R^2 = 0.9947 \text{)}$$

It is important to mention here that the sensitivity of the SnSe/TiO₂@GO-GC electrode toward the oxidation of paracetamol, tryptophan, and caffeine both in the absence and presence of other compounds was nearly the same, which confirms that oxidation processes are independent. Therefore, it is concluded that the proposed electrode is feasible to determine these analytes simultaneously without any interference.

In addition, the order of ability to undergo oxidation, which was evaluated using the peak currents and reaction mechanism, is Para > Caf > Trp. On comparing the oxidation results of Para, Trp, and Caf at the SnSe/TiO₂@GO-GC electrode, the oxidation of Para exhibits a low detection limit and wide linear range. It is due to the easily oxidizable group of phenolic OH. This oxidation is augmented by the N-acyl group at the Para position; although the "NH" lone pair can be shifted and delocalized over the adjacent C=O group before oxidation, it can also be delocalized over the aromatic ring during oxidation. Similarly, Caf oxidation also showed a wide linear range and lowering of potential because it is a simple and compact molecule compared to the flexible Trp, so it can have a strong interaction with the electrode surface and make the concentration range high. In contrast, the indole ring "N" of Trp is expected to have an interaction with the electrode surface. But this interaction is retorted by the amino acid substituent. Hence, the range of concentrations detected was low. The observed results were compared with reported electrodes (Table 1), but the present electrode showed enhanced behavior in terms of a significant increase in peak current and less positive oxidation peak potential value. On the whole, this work forecasts paths for fabrication of numerous composite electrodes with a specific reference to drug determinations in real samples at low overpotentials.

Interference Studies. To demonstrate the selectivity and anti-interference ability of the SnSe/TiO₂@GO-GC electrode, the interference study was carried out for the oxidation of Para, Trp, and Caf with inorganic salts (NaCl, KCl, and CH₃COONa) and organic substances (folic acid, uric acid, dopamine, ascorbic acid, and cysteine). There is no remarkable change in the potential regardless of the organic substances and inorganic salts (Figure S2). This proves the selectivity of the electrode toward the Para, Trp, and Caf oxidations.

Stability, Reproducibility, and Repeatability. The extensive steadiness of the SnSe/TiO₂@GO-GC electrode

Table 1. Representative Electrodes for the Oxidation of Para, Trp, and Caf

modified electrode	analyte	LOD (μM)	linear range (μM)	ref.
activated graphene-Nafion	Para	0.03	0.05–20	48
MWCNT/PSVM/Au/GCE	Para	0.027	0.1–200	49
egg plant	Para	5	20–200	50
CNF-CPE	Trp	1.3	0.1–119	51
Nafion/TiO ₂ -graphene/GCE	Trp	0.7	5–140	52
butyrylcholine/GCE	Trp	0.6	2–60	53
MIS/MWCNTs-VTMS/GCE	Caf	0.22	0.75–40	54
Nafion/GO-GCE	Caf	0.2	0.4–80	55
flavonoid nanostructured GCE	Caf	3.54	10–110	56
GC-SnS/TiO ₂ @GO electrode	Para	0.0075	0.0098–280	previous work ¹¹
	Trp	0.0078	0.013–157	
	Caf	0.0044	0.016–333	
SnSe/TiO ₂ @GO-GC electrode	Para	0.0030	0.0089–410	this work
	Trp	0.0053	0.0136–190	
	Caf	0.0065	0.0160–355	

was investigated by storing the modified electrode in phosphate buffer solution (0.1 M), and even after 10 days of storage, there is no significant decrease in the initial current signal for 50 μL of 10 μM Para, thus endorsing the long-term stability of the modified electrode. In addition, the reproducibility study was carried out for five mutual independent SnSe/TiO₂@GO-GC electrodes and the results showed 1.7% RSD, indicating good reproducibility. Meanwhile, the repeatability studies for the modified electrode were also carried out in the same way for 10 repeated experiments, which result in the RSD of 3.51%, signifying good repeatability (Figure S3). On the whole, these results indicate that the SnSe/TiO₂@GO-GC electrode can be utilized for real applications owing to its outstanding stability, reproducibility, and repeatability.

Real Sample Analysis. An attempt was made to verify the real-time applicability of the SnSe/TiO₂@GO-GC electrode for the detection of paracetamol, tryptophan, and caffeine in human blood serum and pharmaceutical formulations; the samples were collected as mentioned in Experimental Section. The separate electrochemical analysis of samples I, II, and III was carried out in the potential window of 0.2 to 1.5 V with the scan rate of 50 mV s^{-1} , and three consecutive values were recorded with the same procedure (Figure S4). The observed oxidation potentials matched with respective potentials of paracetamol, tryptophan, and caffeine, and Table 2 presents the calculated volumes of the corresponding components. These results are in good agreement with HPLC results (Table 2). The results of both the analytical techniques are commensurable, which prove the real-time application of the SnSe/TiO₂@GO-GC electrode particularly at concomitant determination of paracetamol, tryptophan, and caffeine in serum without any interference.

CONCLUSIONS

In this study, a novel SnSe/TiO₂@GO ternary nanocomposite was prepared through a simplified procedure. The interfacial interaction between the components was confirmed through XRD and XPS spectroscopy. The electrocatalytic activity of the

Table 2. Real Sample Analysis of Paracetamol, Tryptophan, and Caffeine at the SnSe/TiO₂@GO-GC Electrode

sample	composition	spiked/ μM			found ^a / μM			recovery (%)			HPLC method ^a / μM		
		Para	Trp	Caf	Para	Trp	Caf	Para	Trp	Caf	Para	Trp	Caf
I	blood serum												
II	Panadol extra (Para + Caf)	5		0.52	4.96 (± 0.03)	1.39 (± 0.02)	0.53 (± 0.07)	99.2	101	101	4.8 (± 0.03)	1.31 (± 0.03)	0.51 (± 0.07)
	L-tryptophan (500 mg)	5	5		4.9 (± 0.03)	6.5 (± 0.01)		99	101		4.70 (± 0.03)	6.1 (± 0.01)	
III	Paracip-650 (Para)	5											
	L-tryptophan (500 mg)		5			6 (± 0.05)	4.90 (± 0.02)		96.4			6.1 (± 0.05)	
	3 roses			5									4.7 (± 0.02)

^aMean value for $n = 3$.

ternary nanocomposite was demonstrated for simultaneous and separate determination of Para, Trp, and Caf drugs. The comparative results of the SnSe/TiO₂@GO-GC electrode with GO-GC, SnSe-GC, and TiO₂-GC control electrodes showed a significant increase in oxidation peak current and lower overpotential. The enhanced electrocatalytic activity toward the oxidation of analytes may be due to the synergetic effect of the components present in the ternary nanocomposite. The defective nature of GO sheets, the small band gap of SnSe, the high interfacial area of TiO₂, and the attainment of a steady value are collectively responsible for enriched electroactive properties of the SnSe/TiO₂@GO-GC electrode, by which the overpotential decreased with the favorable enhancement in the electron transfer, sensing ability, and selectivity. In addition, wide linear ranges of 0.0089–410, 0.0136–87.66, and 0.0160–355 μM with detection limits of 0.0030, 0.0053, and 0.0065 μM for paracetamol, tryptophan, and caffeine, respectively, were encountered as significant features. This work establishes the real-time application of the SnSe/TiO₂@GO-GC electrode for the simultaneous sensing and determination of paracetamol, tryptophan, and caffeine in pharmaceutical formulations and human blood serum without any interference. Hence, this study can promote interest for the fabrication of high-performance electrochemical sensors for real-time applications in the medical field.

■ ASSOCIATED CONTENT

SI Supporting Information

The Supporting Information is available free of charge at <https://pubs.acs.org/doi/10.1021/acsomega.1c07306>.

Instrumentation details; EDAX spectra of SnSe and the SnSe/TiO₂@GO ternary nanocomposite; elemental mapping of SnSe/TiO₂@GO; deconvoluted XPS spectra of C 1 s, O 1 s, Se 3d, Ti 2p, and Sn 3d; Randles–Sevcik equation; interference, reproducibility, and repeatability results; determination of Para, Trp, and Caf simultaneously in blood serum; HPLC analysis of Para, Trp, and Caf (PDF)

■ AUTHOR INFORMATION

Corresponding Author

Eagambaram Murugan – Department of Physical Chemistry, School of Chemical Sciences, University of Madras, Guindy Campus, Chennai, Tamil Nadu 600025, India; orcid.org/0000-0001-9751-9690; Email: dr.e.murugan@gmail.com

Author

Kalpna Kumar – Department of Chemistry, Dhaanish Ahmed College of Engineering, Chennai, Tamil Nadu 601301, India; orcid.org/0000-0001-7055-9094

Complete contact information is available at: <https://pubs.acs.org/10.1021/acsomega.1c07306>

Author Contributions

E.M. supervised the project and K.K. carried out the experimental work.

Notes

The authors declare no competing financial interest.

ACKNOWLEDGMENTS

The financial assistance provided by DST-PURSE-PHASE II, New Delhi, Government of India, is gratefully acknowledged by the authors.

REFERENCES

- (1) Zhu, M.; Chen, P.; Liu, M. Graphene Oxide Enwrapped Ag/AgX (X = Br, Cl) Nanocomposite as a Highly Efficient Visible-Light Plasmonic Photocatalyst. *ACS Nano* **2011**, *5*, 4529–4536.
- (2) Smith, A. T.; LaChance, A. M.; Zeng, S.; Liu, B.; Sun, L. Synthesis, Properties, and Applications of Graphene Oxide/Reduced Graphene Oxide and Their Nanocomposites. *Nano Mater. Sci.* **2019**, *1*, 31–47.
- (3) Murugan, E.; Kalpana, K. Fabrication of GC-r-GO-PAMAM (G3)-Pd Electrode for Electro-Catalytic Oxidation of Formic Acid. *Adv. Mater. Proc.* **2018**, *3*, 75–81.
- (4) Zhang, Y.; Zhou, Q.; Zhu, J.; Yan, Q.; Dou, S. X.; Sun, W. Nanostructured Metal Chalcogenides for Energy Storage and Electrocatalysis. *Adv. Funct. Mater.* **2017**, *27*, 1702317–1702334.
- (5) Hun, X.; Wang, S.; Mei, S.; Qin, H.; Zhang, H.; Luo, X. Photoelectrochemical Dopamine Sensor Based on a Gold Electrode Modified with SnSe Nanosheets. *Microchim. Acta* **2017**, *184*, 3333–3338.
- (6) Shi, W.; Gao, M.; Wei, J.; Gao, J.; Fan, C.; Ashalley, E.; Li, H.; Wang, Z. Tin Selenide (SnSe): Growth, Properties, and Applications. *Adv. Sci.* **2018**, *5*, 1700602.
- (7) Murugan, E.; Nimita, J.; Ariraman, M.; Rajendran, S.; Kathirvel, J.; Akshata, C. R.; Kumar, K. Core-Shell Nanostructured Fe₃O₄-Poly(Styrene-Co-Vinylbenzyl Chloride) Grafted PPI Dendrimers Stabilized with AuNPs/PdNPs for Efficient Nuclease Activity. *ACS Omega* **2018**, *3*, 13685–13693.
- (8) Yue, J.; Chen, Z. E. Y.; Chen, L.; Zhang, J.; Song, Y.; Zhai, Y. Preparation TiO₂ Core-Shell Nanospheres and Application as Efficiency Drug Detection Sensor. *Nanoscale Res. Lett.* **2014**, *9*, 465–466.
- (9) Siva Prasad, M.; Chen, R.; Ni, H.; Kiran Kumar, K. Directly Grown of 3D-Nickel Oxide Nano Flowers on TiO₂ Nanowire Arrays by Hydrothermal Route for Electrochemical Determination of Naringenin Flavonoid in Vegetable Samples. *Arab. J. Chem.* **2020**, *13*, 1520–1531.
- (10) Murugan, E.; Rubavathy Jaya Priya, A.; Janaki Raman, K.; Kalpana, K.; Akshata, C. R.; Santhosh Kumar, S.; Govindaraju, S. Multiwalled Carbon Nanotubes/Gold Nanoparticles Hybrid Electrodes for Enzyme-Free Electrochemical Glucose Sensor. *J. Nanosci. Nanotechnol.* **2019**, *19*, 7596–7604.
- (11) Murugan, E.; Kumar, K. Fabrication of SnS/TiO₂@GO Composite Coated Glassy Carbon Electrode for Concomitant Determination of Paracetamol, Tryptophan, and Caffeine in Pharmaceutical Formulations. *Anal. Chem.* **2019**, *91*, 5667–5676.
- (12) Mazloum-Ardakani, M.; Sheikh-Mohseni, M. A.; Abdollahi-Alibeik, M.; Benvidi, A. Electrochemical Sensor for Simultaneous Determination of Norepinephrine, Paracetamol and Folic Acid by a Nanostructured Mesoporous Material. *Sens. Actuators, B* **2012**, *171*–*172*, 380–386.
- (13) Murugan, E.; Pakrudheen, I. Efficient Amphiphilic Poly(Propylene Imine) Dendrimer Encapsulated Ruthenium Nanoparticles for Sensing and Catalysis Applications. *Sci. Adv. Mater.* **2015**, *7*, 891–901.
- (14) Taleb, M.; Ivanov, R.; Bereznev, S.; Kazemi, S. H.; Hussainova, I. Alumina/Graphene/Cu Hybrids as Highly Selective Sensor for Simultaneous Determination of Epinephrine, Acetaminophen and Tryptophan in Human Urine. *J. Electroanal. Chem.* **2018**, *823*, 184–192.
- (15) Tang, J.; Liu, Y.; Hu, J.; Zheng, S.; Wang, X.; Zhou, H.; Jin, B. Co-Based Metal-Organic Framework Nanopinnas Composite Doped with Ag Nanoparticles: A Sensitive Electrochemical Sensing Platform for Simultaneous Determination of Dopamine and Acetaminophen. *Microchem. J.* **2020**, *155*, 104759.
- (16) Kulo, A.; Peeters, M. Y.; Allegaert, K.; Smits, A.; de Hoon, J.; Verbesselt, R.; Lewi, L.; van de Velde, M.; Knibbe, C. A. J. Pharmacokinetics of Paracetamol and Its Metabolites in Women at Delivery and Post-Partum. *Br. J. Clin. Pharmacol.* **2013**, *75*, 850–860.
- (17) Camargo, J. R.; Andreotti, I. A. A.; Kalinke, C.; Henrique, J. M.; Bonacin, J. A.; Janegitz, B. C. Waterproof Paper as a New Substrate to Construct a Disposable Sensor for the Electrochemical Determination of Paracetamol and Melatonin. *Talanta* **2020**, *208*, 120458.
- (18) Tajeu, K. Y.; Dongmo, L. M.; Tonle, I. K. Fullerene/MWCNT/Nafion Modified Glassy Carbon Electrode for the Electrochemical Determination of Caffeine. *American journal of analytical chemistry* **2020**, *11*, 114–127.
- (19) Khairy, M.; Mahmoud, B. G.; Banks, C. E. Simultaneous Determination of Codeine and Its Co-Formulated Drugs Acetaminophen and Caffeine by Utilising Cerium Oxide Nanoparticles Modified Screen-Printed Electrodes. *Sens. Actuators, B* **2018**, *259*, 142–154.
- (20) Fooladi, E.; Marzieh, B.; Monireh, R.; Saeid, N. Application of Carboxylic Acid - Functionalized of Graphene Oxide for Electrochemical Simultaneous Determination of Tryptophan and Tyrosine in Milk. *SN Appl. Sci.* **2020**, *2*, 527.
- (21) Wu, Y.; Deng, P.; Tian, Y.; Ding, Z.; Li, G.; Liu, J.; Zuberi, Z.; He, Q. Rapid Recognition and Determination of Tryptophan by Carbon Nanotubes and Molecularly Imprinted Polymer-Modified Glassy Carbon Electrode. *Bioelectrochemistry* **2020**, *131*, 107393.
- (22) Zhang, R.; Jamal, R.; Ge, Y.; Zhang, W.; Yu, Z.; Yan, Y.; Liu, Y.; Abdiryim, T. Functionalized PProDOT@nitrogen-Doped Carbon Hollow Spheres Composites for Electrochemical Sensing of Tryptophan. *Carbon N. Y.* **2020**, *161*, 842–855.
- (23) Wang, Y.; Ouyang, X.; Ding, Y.; Liu, B.; Xu, D.; Liao, L. An Electrochemical Sensor for Determination of Tryptophan in the Presence of Da Based on Poly(L-Methionine)/Graphene Modified Electrode. *RSC Adv.* **2016**, *6*, 10662–10669.
- (24) Wang, C.; Li, Y. D.; Zhang, G. H.; Zhuang, J.; Shen, G. Q. Synthesis of SnSe in various alkaline media under mild conditions. *Inorg. Chem.* **2000**, *39*, 4237–4239.
- (25) Arthi, G. P. B.; BD, L. A Simple Approach to Stepwise Synthesis of Graphene Oxide Nanomaterial. *J. Nanomed. Nanotechnol.* **2015**, *06*, 1–4.
- (26) Shikha, D.; Chauhan, R. P. Comparison of Morphological and Optical Properties of Nanocrystalline Tin Selenide Powder and Thin Films. *Optoelectron. Adv. Mater. Rapid Commun.* **2012**, *2012*, 734–737.
- (27) Moon, I. K.; Lee, J.; Ruoff, R. S.; Lee, H. Reduced Graphene Oxide by Chemical Graphitization. *Nat. Commun.* **2010**, *1*, 73–76.
- (28) Ramasamy, P.; Manivasakan, P.; Kim, J. Phase Controlled Synthesis of SnSe and SnSe₂ Hierarchical Nanostructures Made of Single Crystalline Ultrathin Nanosheets. *CrystEngComm* **2015**, *17*, 807–813.
- (29) Zhang, J.; Boyd, I. W.; Sullivan, B. J. O.; Hurley, P. K.; Kelly, P. V. Nanocrystalline TiO₂ Films Studied by Optical, XRD and FTIR Spectroscopy. *J. Non-Cryst. Solids* **2002**, *303*, 134–138.
- (30) Pejjai, B.; Minnam, R. Eco-Friendly Synthesis of SnSe Nanoparticles: Effect of Reducing Agents on the Reactivity of a Se-Precursor and Phase Formation of SnSe NPs. *New J. Chem.* **2018**, *42*, 4843–4853.
- (31) Sui, R.; Rizkalla, A. S.; Charpentier, P. A. FTIR Study on the Formation of TiO₂ Nanostructures in Supercritical CO₂. *J. Phys. Chem. B* **2006**, *110*, 16212–16218.
- (32) Liu, W.; Cai, J.; Ding, Z.; Li, Z. TiO₂/RGO Composite Aerogels with Controllable and Continuously Tunable Surface Wettability for Varied Aqueous Photocatalysis. *Applied Catal., B* **2015**, *174*–*175*, 421–426.
- (33) Pan, X.; Zhao, Y.; Liu, S.; Korzeniewski, C. L.; Wang, S.; Fan, Z. Nanoparticle Composite Photocatalysts. *ACS Appl. Mater. Interfaces* **2012**, *4*, 3944–3950.
- (34) Jeong, G.; Kim, J.; Gunawan, O.; Pae, S. R.; Kim, S. H.; Song, J. Y.; Lee, Y. S.; Shin, B. Preparation of single-phase SnSe thin-films and

modification of electrical properties via stoichiometry control for photovoltaic application. *J. Alloys Compd.* **2017**, *722*, 474–481.

(35) Wang, Y.; Li, L.; Huang, X.; Lia, Q.; Li, G. Photocatalytic redox catalysts new insights into fluorinated TiO₂ (brookite, anatase and rutile) nanoparticles as efficient photocatalytic redox catalysts. *RSC Adv.* **2015**, *5*, 34302–34313.

(36) Zhang, F.; Xia, C.; Zhu, J.; Ahmed, B.; Liang, H.; Velusamy, D. B.; Schwingenschlöggl, U.; Alshareef, H. N. SnSe₂ 2D Anodes for Advanced Sodium Ion Batteries. *2016*, *6*, 1601188, DOI: 10.1002/aenm.201601188.

(37) Zhao, C.; Cai, Y.; Yin, K.; Li, H.; Shen, D.; Qin, N.; Lu, Z.; Liu, C.; Wang, H. E. Carbon-bonded, oxygen-deficient TiO₂ nanotubes with hybridized phases for superior Na-ion storage. *Chem. Eng. J.* **2018**, *350*, 201–208.

(38) Zhang, W.; Yang, Z.; Liu, J.; Zhang, L.; Hui, Z.; Yu, W.; Qian, Y.; Chen, L.; Liu, X. Room Temperature Growth of Nanocrystalline Tin (II) Selenide from Aqueous Solution. *J. Cryst. Growth* **2000**, *217*, 157–160.

(39) Cai, Y.; Wang, H.-E.; Zhao, X.; Huang, F.; Wang, C.; Deng, Z.; Li, Y.; Cao, G.; Su, B.-L. Walnut-like Porous Core / Shell TiO₂ with Hybridized Phases Enabling Fast and Stable Lithium Storage. *CS Appl. Mater. Interfaces* **2017**, *9*, 10652–10663.

(40) Han, Y.-M.; Zhao, J.; Zhou, M.; Jiang, X.-X.; Leng, H.-Q.; Li, L.-F. Thermoelectric Performance of SnS and SnS – SnSe Solid Solution. *J. Mater. Chem. A* **2015**, *3*, 4555–4559.

(41) Mahmoud, B. G.; Khairy, M.; Rashwan, F. A.; Banks, C. E. Simultaneous Voltammetric Determination of Acetaminophen and Isoniazid (Hepatotoxicity-Related Drugs) Utilizing Bismuth Oxide Nanorod Modified Screen-Printed Electrochemical Sensing Platforms. *Anal. Chem.* **2017**, *89*, 2170–2178.

(42) Chrzescijanska, E.; Wudarska, E.; Kusmierek, E.; Rynkowski, J. Study of Acetylsalicylic Acid Electroreduction Behavior at Platinum Electrode. *J. Electroanal. Chem.* **2014**, *713*, 17–21.

(43) Laviron, E. General Expression of the Linear Potential Sweep Voltammogram in the Case of Diffusionless Electrochemical Systems. *J. Electroanal. Chem.* **1979**, *101*, 19–28.

(44) García-Miranda Ferrari, A.; Foster, C. W.; Kelly, P. J.; Brownson, D. A.; Banks, C. E. Determination of the Electrochemical Area of Screen-Printed Electrochemical Sensing Platforms. *Biosensors* **2018**, *8*, 53.

(45) Lima, A. B.; Torres, L. M. F. C.; Guimarães, C. F. R. C.; Verly, R. M.; Da Silva, L. M.; Carvalho Júnior, A. D.; Dos Santos, W. T. P. Simultaneous Determination of Paracetamol and Ibuprofen in Pharmaceutical Samples by Differential Pulse Voltammetry Using a Boron-Doped Diamond Electrode. *J. Braz. Chem. Soc.* **2014**, *25*, 478–483.

(46) Yokogoshi, H.; Tani, S.; Amano, N. The Effects of Caffeine and Caffeine-Containing Beverages on the Disposition of Brain Serotonin in Rats. *Agric. Biol. Chem.* **1987**, *51*, 3281–3286.

(47) Babaei, A.; Ansari, E.; Afrasiabi, M. A New Sensor Based on a MCM-41-Nickel Hydroxide Nanoparticle-Multi-Walled Carbon Nanotube-Modified Glassy Carbon Electrode for a Sensitive Simultaneous Determination of Levodopa, Paracetamol and Tryptophan. *Anal. Methods* **2014**, *6*, 8729–8737.

(48) Kim, D.; Lee, S.; Piao, Y. Electrochemical Determination of Dopamine and Acetaminophen Using Activated Graphene-Nafion Modified Glassy Carbon Electrode. *J. Electroanal. Chem.* **2017**, *794*, 221–228.

(49) Liu, J.; Xie, Y.; Wang, K.; Zeng, Q.; Liu, R.; Liu, X. A Nanocomposite Consisting of Carbon Nanotubes and Gold Nanoparticles in an Amphiphilic Copolymer for Voltammetric Determination of Dopamine, Paracetamol and Uric Acid. *Microchim. Acta* **2017**, *184*, 1739–1745.

(50) Garcia, L. F.; Benjamin, S. R.; Antunes, R. S.; Lopes, F. M.; Somerset, V. S.; Gil, E. d. S. Solanum Melongena Polyphenol Oxidase Biosensor for the Electrochemical Analysis of Paracetamol. *Prep. Biochem. Biotechnol.* **2016**, *46*, 850–855.

(51) Tang, X.; Liu, Y.; Hou, H.; You, T. Electrochemical Determination of L-Tryptophan, L-Tyrosine and L-Cysteine Using

Electrospun Carbon Nanofibers Modified Electrode. *Talanta* **2010**, *80*, 2182–2186.

(52) Fan, Y.; Liu, J. H.; Lu, H. T.; Zhang, Q. Electrochemistry and Voltammetric Determination of L-Tryptophan and L-Tyrosine Using a Glassy Carbon Electrode Modified with a Nafion/TiO₂-Graphene Composite Film. *Microchim. Acta* **2011**, *173*, 241–247.

(53) Jin, G. P.; Lin, X. Q. The Electrochemical Behavior and Amperometric Determination of Tyrosine and Tryptophan at a Glassy Carbon Electrode Modified with Butyrylcholine. *Electrochem. Commun.* **2004**, *6*, 454–460.

(54) De Jesus, W.; Santos, R.; Santhiago, M.; Valeria, I.; Yoshida, P.; Tatsuo, L. Electrochemical Sensor Based on Imprinted Sol – Gel and Nanomaterial for Determination of Caffeine. *Sens. Actuators, B* **2012**, *166–167*, 739–745.

(55) Zhao, F.; Wang, F.; Zhao, W.; Zhou, J.; Liu, Y.; Zou, L.; Ye, B. Voltammetric Sensor for Caffeine Based on a Glassy Carbon Electrode Modified with Nafion and Graphene Oxide. *Microchim. Acta* **2011**, *174*, 383–390.

(56) Amiri-aref, M.; Raoof, J. B.; Ojani, R. A Highly Sensitive Electrochemical Sensor for Simultaneous Voltammetric Determination of Noradrenaline, Acetaminophen, Xanthine and Caffeine Based on a Flavonoid Nanostructured Modified Glassy Carbon Electrode. *Sens. Actuators, B* **2014**, *192*, 634–641.